Published in final edited form as:
J Mol Cell Cardiol. 2010 January ; 48(1): 191. doi:10.1016/j.yjmcc.2009.07.017.

DIFFERENTIAL EFFECTS OF THE TRANSIENT OUTWARD K+ CURRENT ACTIVATOR NS5806 IN THE CANINE LEFT VENTRICLE

Kirstine Calloe, PhD[2], **Ewa Soltysinska, MSc**[2], **Thomas Jespersen, PhD**[2], **Alicia Lundby, PhD**[2], **Charles Antzelevitch, PhD**[1], **Søren-Peter Olesen, MD, PhD**[2], and **Jonathan M Cordeiro, PhD**[1]

[1]Department of Experimental Cardiology, Masonic Medical Research Laboratory Utica, New York, USA 13501

[2]Danish National Research Foundation Center for Cardiac Arrhythmias Dep. of Biomedical Sciences 12.5.10 University of Copenhagen Blegdamsvej 3 DK-2200 Copenhagen N Denmark

Abstract

Objective: To examine the electrophysiological and molecular properties of the transient outward current (I_{to}) in canine left ventricle using a novel I_{to} activator, NS5806.

Methods and Results: I_{to} was measured in isolated epicardial (Epi), midmyocardial (Mid) and endocardial (Endo) cells using whole-cell patch-clamp techniques. NS5806 activation of $K_V4.3$ current was also studied in CHO-K1 cells and *Xenopus laevis* oocytes. In CHO-K1 cells co-transfected with $K_V4.3$ and KChIP2, NS5806 (10 μM) caused a 35 % increase in current amplitude and a marked slowing of current decay with τ increasing from 7.0±0.4 to 10.2±0.3 ms. In the absence of KChIP2, current decay was unaffected by NS5806. In ventricular myocytes, NS5806 increased I_{to} density by 80%, 82%, and 16% in Epi, Mid, and Endo myocytes, respectively (at +40 mV) and shifted steady-state inactivation to negative potentials. NS5806 also significantly slowed decay of I_{to}, increasing total charge to 227%, 192% and 83% of control in Epi, Mid and Endo cells, respectively (+40 mV, $p<0.05$). Quantification of $K_V4.3$ and KChIP2 mRNA in the 3 ventricular cell types revealed that levels of $K_V4.3$ message was uniform but those of KChIP2 were significantly greater in Epi and Mid cells. The KChIP2 gradient was confirmed at the protein level by Western blot.

Conclusions: Our results suggest that NS5806 augments I_{to} by increasing current density and slowing decay and that both depend on the presence of KChIP2. I_{to} and its augmentation by NS5806 are greatest in Epi and Mid cells because KChIP2 levels are highest in these cell types.

Keywords

ventricular muscle; transient outward K^+ channel; repolarization; heterogeneity

Corresponding author: Jonathan M Cordeiro, Ph.D. Masonic Medical Research Laboratory 2150 Bleecker Street Utica, NY 13501 U.S.A. Phone: (315) 735-2217 x132 Fax: (315) 735-5648 jcordeiro@mmrl.edu.

Conflicts of Interest: Søren-Peter Olesen is consultant to NeuroSearch.

INTRODUCTION

Repolarization of the cardiac action potential is initiated and controlled by activation of a number of time- and voltage-dependent K^+ currents. In dog heart at least four K^+ currents play important roles in regulating the cardiac action potential duration: (i) a Ca^{2+}-independent transient outward K^+ current (I_{to}); (ii) an inwardly rectifying K^+ current (I_{K1}) and (iii) the rapid and slow forms of the delayed rectifier K^+ current (I_{Kr} and I_{Ks}, respectively). An I_{to} has been identified in the myocardium of most mammalian species (for review see [1]). Ventricular epicardial (Epi) tissue has a more prominent I_{to} compared to endocardial (Endo) tissue [2-5]. Recently, it has been demonstrated that I_{to} can be modulated by several proteins such as K^+-channel interacting protein (KChIP) [6,7], IRX [8], calcineurin/NFAT [9], DPP's [10] and various KCNE subunits [11,12].

Although an I_{to} gradient between Epi and Endo has been identified, the precise molecular identity of I_{to} in the canine ventricular myocardium remains unclear. It is generally believed that $K_V4.3$ channels comprise the majority of transient outward K^+ channels in canine heart [13]. Previous studies have also identified $K_V1.4$ and $K_V1.5$ gene products in ventricular tissue [13,14]. However, the precise role of these alpha subunits and their contribution to canine I_{to} remains to be determined. Recent evidence also suggests that several β-subunits including KChIP2 can alter peak $I_{Kv4.3}$ density, slow decay of the current and accelerate recovery from inactivation[7]. However, the relative abundance of $K_V4.3$ and KChIP2 in canine ventricle remains controversial. Several studies suggest that $K_V4.3$ levels are uniform throughout the canine left ventricle and the gradient in I_{to} expression is due to a gradient in KChIP2 [15,16]. In contrast, another study found that KChIP2 protein was uniform throughout the left ventricle suggesting that I_{to} gradient in ventricle is not due to a gradient in KChIP2 levels [7]. Finally, Zicha et al. [17] found that both $K_V4.3$ and KChIP2 exhibit a transmural gradient, with Epi expression being greater than Endo expression in canine ventricle.

The present study compares the electrophysiological and molecular properties of the Ca^{2+}-independent transient outward K^+ currents in single myocytes isolated from the canine left ventricle. Results of our study indicate that the biophysical and molecular properties of I_{to} differ significantly in endocardial cells compared to midmyocardial (Mid) or epicardial cells. Analysis of the molecular subunits revealed that KChIP2 mRNA levels are lower in the endocardium, contributing to some of the observed biophysical differences. Furthermore, we found that the levels of putative I_{to} subunits $K_V4.3$ and $K_V1.4$ are equally distributed throughout the left ventricle. Utilizing the I_{to} activator, NS5806 [18], we confirm by pharmacological methods that KChIP2 is functionally important for I_{to} activation and that KChIP2 levels are lower in endocardial cells. Application of this I_{to} activator resulted in a significant increase in I_{to}, with the greatest effect observed in Epi and Mid cells. The regional variations in subunit contribution are responsible for the observed biophysical differences in magnitude and kinetics of I_{to}.

METHODS

Expression of $K_V4.3$ and KChIP2 in CHO-K1—Human (h) $K_V4.3$ (NM_172198) and hKChIP2.1 (NM_173192) were transiently expressed in CHO-K1 in a 1:3 molar ratio using Lipofectamine and Plus Reagent according to manufacturer's instruction (GIBCO, Invitrogen). The cells were cultured in Dulbecco's modified Eagle's medium (DMEM, Substrate Department, University of Copenhagen, Denmark) supplemented with 10% fetal calf serum (GIBCO, Invitrogen) and 40 mg/L L-Proline at 37°C in 5% CO_2.

Expression of $K_V4.3$ and KChIP2 in *Xenopus laevis* oocytes—Female *Xenopus laevis* frogs were anaesthetized with Tricain (2 g/l, Sigma) and ovarian lobes were removed.

Oocytes were defolliculated enzymatically in 1% collagenase (Boehringer Mannheim) and 0.1% trypsin inhibitor (Sigma) in Kulori solution for 1 h followed by wash in Kulori containing 0.1% BSA (Sigma).

cRNA was prepared from $hK_v4.3$ and hKChIP2.1 using the mMESSAGE mMACHINE T7 kit (Ambion). 50 nl cRNA was injected using a Nanoject microinjector (Drummond Scientific, Broomall, PA) in molar ratios of $K_v4.3$ and KChIP2. The concentration of $K_v4.3$ was kept constant at 0.1 ng. Oocytes were kept at 19°C and currents measured 2 days after injection.

Isolation of adult myocytes—Myocytes from Epi, Endo and Mid regions were prepared from canine hearts using techniques previously described [19,20]. Adult mongrel dogs were anesthetized with sodium pentobarbital (35 mg/kg i.v.), their hearts were rapidly removed and placed in nominally Ca^{2+}-free Tyrode's solution. A wedge consisting of the left ventricular free wall was cannulated and perfused with nominally Ca^{2+}-free Tyrode's solution containing 0.1% BSA for about 5 minutes. The wedge preparations were then subjected to enzyme digestion with the nominally Ca^{2+}-free solution supplemented with 0.5 mg/ml collagenase (Type II, Worthington), 0.1 mg/ml protease (Type XIV, Sigma) and 1 mg/ml BSA for 8-12 minutes. After perfusion, thin slices of tissue from the Epi (<2 mm from the epicardial surface), Mid (about 5-7 mm from the epicardial surface), and Endo (<2 mm from the endocardial surface) were shaved from the wedge using a dermatome. The tissue slices were then placed in separate beakers minced and incubated in fresh buffer containing 0.5 mg/ml collagenase, 1 mg/ml BSA and agitated. The supernatant was filtered, centrifuged at 200 rpm for 2 minutes and the pellet containing the myocytes was stored in 0.5 mM Ca^{2+} HEPES buffer at room temperature.

Solutions—$K_v4.3$ currents in CHO-K1 was measured using an extracellular NaCl Ringer solution (mM): NaCl 140, KCl 4, $CaCl_2$ 2, $MgCl_2$ 1, HEPES 10, pH=7.4 adjusted with NaOH and an intracellular solution (mM): KCl 110, KOH/EDTA 31/10, $CaCl_2$ 5.17, $MgCl_2$ 1.42, HEPES 10, MgATP 4, pH=7.2 with KOH. Kulori solution contained (mM): NaCl 90, KCl 4, $MgCl_2$ 1, $CaCl_2$ 1, HEPES 5, pH=7.4 with NaOH. The nominally Ca^{2+}-free dissecting buffer contained (mM): NaCl 129, KCl 5.4, $MgSO_4$ 2.0, NaH_2PO_4 0.9, glucose 5.5, $NaHCO_3$ 20 and was bubbled with 95% O_2/5% CO_2. Ventricular cells were superfused with HEPES buffer (mM): NaCl 126, KCl 5.4, $MgCl_2$ 1.0, $CaCl_2$ 2.0, HEPES 10, glucose 11, pH=7.4 with NaOH. The pipette solution consisted of (mM): K-aspartate 90, KCl 30, glucose 5.5, $MgCl_2$ 1.0, EGTA 5, MgATP 5, HEPES 5, NaCl 10, pH=7.2 with KOH.

Electrophysiology—I_{to} recordings from myocytes were performed as previously described [21]. All myocyte and CHO-K1 experiments were performed at 36°C. Voltage-clamp and conventional recordings were made using a MultiClamp 700A amplifier and MultiClamp Commander (Axon Instruments). Patch pipettes were fabricated from borosilicate glass capillaries (1.5 mm O.D., Fisher Scientific, Pittsburg, PA). Pipettes were pulled using a gravity puller (Narishige Corp) and the resistance ranged from 0.9-3 MΩ when filled with the internal solution. Cell capacitance was measured by applying −5 mV voltage steps. Electronic compensation of series resistance to 60-70% was applied. All analog signals were acquired at 10-25 kHz, filtered at 4-6 kHz, digitized with a Digidata 1322 converter (Axon Instruments) and stored using pClamp9 software.

Recordings from oocytes were performed using a two-electrode voltage-clamp amplifier (Dagan CA-1B; Chicago, IL). Borosilicate glass recording electrodes (Module Ohm, Denmark) were made using a DMZ-Universal Puller (Zeitz Instruments, Germany) and had a resistance of 0.5 to 1 MΩ when filled with 2 M KCl. Oocytes were superfused with Kulori solution and experiments performed at room temperature.

Analysis of mRNA Levels in the Left Ventricle

RNA preparation and cDNA synthesis—RNA was prepared from canine left ventricular tissue. Tissue samples were shaved using a dermatome and stored in an RNA stabilizing solution (RNAlater®-ICE, Ambion). Total RNA was purified from the homogenized tissue specimens (homogenizer Kinemtica, Buch & Holm, Switzerland) with Tri Reagent® (Sigma-Aldrich) according to the manufacturer's instructions. Total cDNA was synthesized from 2 μg total RNA using the High-Capacity cDNA Reverse Transcription Kit (Applied Biosystem) with random hexamer primers following the manufacturer's instructions.

Real-time PCR—Real-time reverse transcriptase-polymerase chain reaction (RT-PCR) was performed on the 7300 RT-PCR System (Applied Biosystem) and data were collected by SDS1.2 software. The selected genes were investigated using TaqMan assays (TaqMan® MGB probe and primers). The pre-designed gene expression assays from Applied Biosystems were as follows: cf02698011 (*KCND3*), cf02624497 (*KCNIP2*), cf02640342 (*DPP10*), cf02690512 (*KCNE1*), cf02625138 (*KCNE2*), cf02646775 (*KCNE3*), cf02650669 (*KCNE4*), cf02698674 (*IRX5*), cf02657295 (*SMYD1*), cf0263023048 (*KCNA5*), cf02659079 (*β2-microglobulin*), and cf02629556 (*Cyclophilin B*). The primers and probes targeting *KCND2, KCNA4, KCNE5, DPP6*, and *HPRT* were designed and synthesized by Applied Biosystems, following submission of intron spanning sequences using Primer Express 3.0 software. Thermal profile for all the real-time PCR reactions was as followed: 50°C (2 min), 95°C (10 min) and then 40 cycles with 95°C (15 sec) and 60°C (1 min).

Prior to the experiments, PCR efficiency for each assay was calculated using a standard curve constructed by plotting range of log cDNA input against Ct (threshold cycle) value. The slope of the plot was used to calculate the percentage amplification efficiency (PE). PE values ranged between 90% and 110% and an amplification efficiency of 2 (100%) per cycle has therefore been used in all the calculations. For each tissue specimen, each gene was quantified in triplicates. Three reference genes were tested: *Cyclophilin B, HPRT*, and *β2-microglobulin*. Quantification of these three genes gave almost similar result and *Cyclophilin B* was chosen for normalization. Normalized gene expression levels were calculated by the $2^{\Delta\Delta Ct}$ method [22]. Delta cycle threshold (ΔC_t) values were calculated by subtracting the Ct value of a target gene from the Ct value of *Cyclophilin B* for each sample. Values for the relative expression were obtained by using the following formula: $1/(2^{-\Delta Ct})*100$.

Western blotting—Epi, Mid and Endo tissue from 5 dogs was snap-frozen in liquid nitrogen and stored in −80 C prior to protein isolation. Total membrane and cytosolic proteins were isolated using a method modified after Han et al. [23]. Briefly, the tissue (20-30 mg) was pulverized in liquid nitrogen and suspended in 500 μL of ice-cold TE buffer (containing Tris 20 mM, EDTA 1 mM supplemented with a cocktail of protease inhibitors: 10 μM 4-(2-aminoethyl)benzenesulphonyl fluoride, 0.2 μM leupeptin, 0.4 μM bestatin, 0.15 μM pepstatin A, 0.14 μM M E-64 and 8 pM aprotinin, all from Sigma). The tissue suspension was treated with 2% of Triton X-100 for 2 hours at 4°C, centrifuged at 15 000 g for 15 minutes at 4°C. The soluble fraction was retained and stored in −80 C prior to Western blotting. Protein concentration was measured (in triplicates for each sample) using Bradford method (DC Protein Assay, Sigma). Samples (50 μg/lane) were separated on precast polyacrylamide 4-15% SDS-PAGE gels (BioRad) at 100 V for 2 hours and transferred to hybond-P PVDF membranes (Amersham Biosciences, 0.45 μm) at 400 mA for 2 hours. Membranes were blocked with 5% non-fat milk in TBST (Tris 10 mM, NaCl 150 mM, 0.1% Tween 20, pH=7.4) for 1-2 hour at RT and then incubated overnight at 4°C in monoclonal antibody against KChIP2b (1:200, clone K60/73, obtained from NeuroMab Facility, supported by NIH grant U24NS050606 and maintained by the Department of Pharmacology, School of Medicine, University of California, Davis, CA 95616). The proteins were detected by HRP-conjugated donkey anti-mouse

antibody (1/10000, Jackson Immunosearch Laboratories) and visualized by ECL staining (Supersignal West Pico Chemiluminescent detection system, Pierce). Immunoblots were exposed (for 5-10 minutes) on hyperfilm ECL (Amersham Biosciences). To assess equal loading, the membranes were stripped in Restore™ Western Blot Stripping Buffer (Pierce) for 20 minutes in RT and re-probed with a mouse anti-actin antibody (MAB1501, Chemicon International). Band density was quantified by Quantity-One software as Gaussian trace quantity. KChIP2 signal was detected as two bands with molecular weight between about 25-32 kDa.

Statistics—Pooled data are presented as Mean±SEM. Statistical analysis was performed using an ANOVA test followed by a Student-Newman-Keuls test or Student t-test, as appropriate, using SigmaStat software. Statistical analysis of RNA and protein expression was performed with a repeated measures ANOVA followed by a Tukey's post test. $p<0.05$ was considered statistically significant.

RESULTS

Our previous studies showed that NS5806 activated native I_{to} in canine ventricular tissue [18]. To address the mechanism of this activation, we tested the effect of the compound on $K_V4.3$ channels transiently expressed in CHO-K1 cells. As an initial basis of comparison, the enhancement of $I_{Kv4.3}$ by NS5806 (10 μM) was determined in the absence and presence of KChIP2 (Figure 1). Application of NS5806 to CHO-K1 cells expressing $K_V4.3$ and KChIP2 resulted in a 35 % increase in $I_{Kv4.3}$ peak current amplitude and a dramatic slowing in decay (τ), from 7.0±0.4 to 10.2±0.3 ms (Figure 1A-C). In contrast, application of NS5806 to CHO-K1 cells expressing only $K_V4.3$ did not change peak $I_{Kv4.3}$ (Figure 1A-B). The decay of the current was unaffected over a range of potentials (Figure 1C). These results suggest that NS5806 can be used to discriminate between currents mediated by $K_V4.3$ alone and $K_V4.3$ together with KChIP2 as the effect of NS5806 is dependent on the presence of KChIP2. We next evaluated the effect on steady state gating parameters using a prepulse-test pulse voltage clamp protocol (Figure 1D). Peak current following a 0.5 sec prepulse was normalized to the maximum current and plotted as a function of the prepulse voltage to obtain the availability of the channels and a Boltzmann function was fitted to the data. NS5806 caused a significant negative shift in the mid-inactivation voltage for $K_V4.3$ from −51.6±0.8 to −60.7±0.8 and the respective slope factors were k=−6.8±0.7 and k=−6.4±0.7 (not significant). For $K_V4.3$ in the presence of KChIP2, mid-inactivation significantly shifted from −38.6±0.1 to −43.6±0.3 mV and the respective slope factors were significantly different with k=−5.1±0.1 and k=−6.3±0.2 (Figure 1D). Recovery from inactivation was addressed by a double-pulse protocol (Figure 1E). For $K_V4.3$ channels the time constant (τ) was significantly slowed from τ =47.7±3.6 ms to 74.0±7.7 ms in the presence of NS5806. Similar results were found for $K_V4.3$ in the presence of KChIP2, where NS5806 slowed the recovery from τ=6.1±0.5 ms to 22.8±1.5ms.

The enhancement of $I_{Kv4.3}$ as well as the slowing of $I_{Kv4.3.}$ decay appeared to be dependent on KChIP2 and previous studies have suggested a differential distribution of KChIP2 levels across the canine left ventricle [15,16] In the next series of experiments, the effect of NS5806 on *Xenopus laevis* oocytes injected with different ratios of $K_V4.3$ and KChIP2 was evaluated (Figure 2). Application of N S5806 resulted in a significant increase in peak current by 12.1, 5.9 and 11.8% in channels with 4:2, 4:4, and 4:12 ratios respectively (Figure 2A) and resulted in a significant slowing of current decay only in the presence of KChIP2 (Figure 2B). This resulted in an increase in charge movement (Figure 2C). The effect of KChIP2 appeared to saturate at a 4:4 cRNA ratio.

The data obtained on K_V 4.3 expressed in CHO-K and *Xenopus laevis* oocytes could suggests that NS5806 can be used to discriminate whether KChIP2 is present in native I_{to} channels as

$K_V4.3$ current decay was slowed by NS5806 only when KChIP2 was co-expressed. Thus if $K_V4.3$ and KChIP2 interact in ventricular cardiomyocytes we would expect an increase in current and a slowing of the decay. We next determined the effect of the I_{to} activator NS5806 in Epi Mid and Endo cardiomyocytes. The density of I_{to} was examined in the absence and presence of 10 μM NS5806. Cd^{2+} (300 μM) was added to the extracellular solution to block the calcium current (I_{CaL}). Following a brief step to −50 mV to discharge sodium channels, voltage steps from −40 to +50 mV applied to all three cell types elicited fast activating and rapidly inactivating I_{to} currents. Representative currents measured in Epi and Endo are shown in Figure 3A-B. Application of NS5806 resulted in an increase in the magnitude of I_{to} as well as slowing the decay of the current. Analysis of the current-voltage (I-V) relation of peak I_{to} showed that the current density was significantly greater in Epi and Mid cells compared to Endo, as previously reported [3,17]. Application of 10 μM NS5806 significantly increased the peak current amplitude of I_{to} in Epi and Mid cells but had no effect in Endo cells (Figures 3C-E). Evaluation of I_{to} in ventricular myocytes showed that application of NS5806 increased the magnitude of current by 80%, 82%, and 16% in Epi, Mid, and Endo myocytes, respectively (at +40 mV).

The time constant of decay (τ) of I_{to} following application of NS5806 was significantly slower in all 3 cell layers (Figure 4A-C). This slowing of I_{to} coupled with the increase in current magnitude resulted in a marked increase in total charge (assessed as area under the current trace, Figure 4D-F). While the area was significantly increased in all 3 cell layers, Epi and Mid cells showed the greatest effect. NS5806 increased total charge by 227%, 192% and 83% compared to control in Epi, Mid, and Endo cells respectively (at +40 mV, $p<0.05$).

We next determined if the difference in current density between the three cell types was due to changes in steady state gating parameters. Steady state inactivation of I_{to} was evaluated using a prepulse-test pulse voltage clamp protocol (top of Figure 5) in presence of Cd^{2+}. The peak current following a 2 sec prepulse was normalized to the maximum current and plotted as a function of the prepulse voltage to obtain the availability of the channels and a Boltzmann function was fitted to the data. In the absence of drug, the mid-inactivation voltage and slope factors were −46.0±1.0 mV, k=4.75±0.44 for Epi (Figure 5C), −43.7±0.8 mV, k=4.17±0.41 for Mid (Figure 5D) and −52.9±1.1, k=8.45±1.34 mV for Endo cells (Figure 5E). Application of NS5806 (10 μM) caused a significant shift in the mid-inactivation potential in all cell layers with mid-inactivation voltage and slope factors of −52.0±0.9 mV, k=4.18±0.37 for Epi (Figure 5C), −48.7±0.7 mV, k=4.04±0.59 for Mid (Figure 5D) and −56.3±0.8 mV, k=7.73±1.07 for Endo cells (Figure 5E). The mid-inactivation potential of I_{to} is significantly shifted to more negative potentials and this shift could not account for the increase in current magnitude observed in the presence of NS5806.

We next tested if I_{to} recovery from inactivation was different in the three ventricular cell layers. Representative traces of the frequency-dependent changes in I_{to} in the absence and presence of NS5806 are shown in Figure 6A-B. Reactivation of I_{to} at −80 mV for all three cell types showed a fast and a slow phase of recovery as follows: i) τ1=43.8±6.7 ms and τ2=256.6±18.9 ms for Epi cells, ii) τ1=39.7±8.3 ms and τ2=278.4±19.2 ms for Mid, and iii) τ1=75.2±8.6 ms and τ2=803.9±79.8 ms for Endo (Figure 6C-E). In addition, under control conditions (absence of NS5806) the recovery of I_{to} was much slower in Endo cells compared to Epi and Mid cells. In the presence of NS5806, the reactivation of I_{to} in Epi and Mid cells could be fit with a single exponential and was markedly faster with τ=55.6±1.7 ms for Epi and τ=71.3±2.8 ms for Mid (Figure 6C-D). However, in the presence of NS5806 reactivation time course of I_{to} in Endo cells was unchanged with τ1=87.2±8.2 ms and τ2=705.6±81.8 ms (Figure 6E).

The differential effects of the I_{to} activator in the 3 ventricular cell layers could suggest that KChIP2 levels may be high in Epi and Mid cells and low in Endo tissue corresponding to the

effects of NS5806 on $K_v4.3$ expressed with different ratios of KChIP2 (Figure 2). However, as KChIP2 slows $K_v4.3$ current decay and the decay of Endo I_{to} is slower than that of Epi and Mid (Figure 4), it seems unlikely that transmural differences in I_{to} kinetics, and response to NS5806 is solely due to differential KChIP2 expression. Other K_v channel subunits may contribute to I_{to}, in particular in Endo tissue. To test this hypothesis, the expression level of the genes encoding proteins suspected to mediate I_{to} as well as I_{Kur} was investigated (Figure 7). The relative mRNA expression levels of *KCND2* and *KCND3*, encoding $K_v4.2$ and $K_v4.3$, respectively, showed an almost 10,000-fold higher expression of *KCND3* as compared to *KCND2*, demonstrating that $K_v4.3$ is the predominant α-subunit. We also tested the expression of several ancillary subunits and found a high expression of *KChIP2*, *DPP6* and *KCNE1*. *DPP6* was found to be expressed in an approximately 100-fold higher level than *DPP10*. For the KCNE β-subunits, *KCNE1* mRNA was expressed at a high level, *KCNE2-4* in intermediate levels, and *KCNE5* at a low level. The expression of 2 transcription factors, *SMYD1* and *IRX5*, believed to be important for the I_{to} gradient in other species [24,25] was also investigated. *SMYD1* (Bop) transcripts were found in a much higher abundance than *IRX5* transcripts. *KCNA4* ($K_v1.4$) and *KCNA5* ($K_v1.5$) transcripts were found to be expressed in 10% and 30-50%, respectively, of the level of *KCND3* ($K_v4.3$).

Transmural differences in the expression level were found for several genes (Figure 8). As reported previously, there was no gradient for *KCND3* and a large gradient for *KCNIP2* with higher expression in the EPI compared to the ENDO [15,16]. For *DPP6* a difference in expression level was observed between Epi and Mid, with more transcript in the Mid. For both the transcription factors *IRX5* and *SMYD1* a higher expression level was found in Endo compared to the Epi consistent with suggested function as negative regulators of expression of I_{to} related genes.

The transmural gradient of KChIP2 transcript was paralleled at protein level as assessed by Western blotting (Figure 8). We repeatedly obtained two bands, using three other different methods of protein purification (data not shown). Antigenic peptide could not be obtained to assess the specificity of the KChIP2 signal but no unspecific bands were found in HEK-293 cell lysate. As the KChIP2 antibody was raised against a highly conserved region, the two bands could represent different KChIP2 splice variants as previously reported in cardiac tissue [26] and both bands were quantified (Figure 8).

DISCUSSION

Summary of Main Findings

In CHO-K1 cells and in *Xenopus laevis* oocytes, the effect on $I_{Kv4.3}$ decay by NS5806 was dependent on the presence of KChIP2. In the presence of KChIP2, application of NS5806 increased peak current and slowed current decay. This was reflected as a significant increase in total charge movement in the presence of KChIP2. In canine ventricular cells, Endo I_{to} was smaller, the decay significantly slower, mid-inactivation voltage was more negative and the recovery from inactivation substantially slower when compared to Mid and Epi I_{to}. Application of NS5806 caused an increase in the magnitude of Mid and Epi I_{to} but had no effect on Endo I_{to} magnitude. In all three layers, the decay of the current was slowed. In the presence od NS5806, recovery from inactivation was faster in Mid and Epi cells but reactivation of Endo I_{to} was unaffected. These observations could suggest that different subunits contribute to Endo I_{to}.

Analysis of mRNA expression levels of putative I_{to} subunits across the canine left ventricular wall revealed a differential distribution of KChIP2 levels with Endo tissue expressing the lowest levels. $K_v4.3$ levels appeared uniform and no other putative subunits exhibited a

transmural gradient. These results suggest that a KChIP2 gradient is responsible for the I_{to} gradient observed in the canine left ventricle.

Molecular Identification of I_{to} in the Left Ventricle

The precise molecular identity of I_{to} in the canine ventricular myocardium remains unclear. It is generally believed that $K_v4.3$ channels comprise the majority of transient outward K^+ channels in canine heart with lower levels of $K_v1.4$ also being identified [13,27]. Recent evidence suggests that several β-subunits including KChIP2 can alter peak $I_{Kv4.3}$ density, slow decay of the current and accelerate recovery from inactivation [7]. However, the relative abundance of $K_v4.3$ and KChIP2 in canine ventricle remains controversial. Our qPCR results confirm that the I_{to} gradient across the left ventricle is likely due to a KChIP2 gradient which was also confirmed at protein level. We also investigated if other putative I_{to} subunits exhibited a transmural gradient but found no significant differences. For *KCNE1* and *KCNE3* there was a tendency toward higher expression in Endo compared to Mid and Epi. In CHO-K1 cells, KCNE1 did not significantly affect $K_v4.3$ + KChIP2 current amplitude [12] whereas in HEK cells, KCNE1 has been demonstrated to increase $K_v4.3$ currents [28] and thus is an unlikely candidate responsible for the I_{to} gradient. KCNE3 has been demonstrated to inhibit $K_v4.3$ ±KChIP2 current [29,30] which is consistent with the smaller I_{to} in Endo.

We also observed the presence of $K_v1.4$ mRNA, in agreement with previous experiments [13]. Interestingly, results of our molecular analysis revealed the presence of $K_v1.5$ mRNA in higher amounts than that of $K_v1.4$ as previously reported [13]. While it has been shown that $K_v1.5$ is abundantly expressed in the atria and is thought to mediate I_{Kur} [31], recent studies have suggested that I_{Kur} is also present in ventricle [14]. If Kv1.4 and Kv1.5 contribute to I_{to}, then the relative contribution of $K_v1.4$ and $K_v1.5$ may be of greater importance in Endo where KChIP2 mRNA levels are low and the contribution of current generated by $K_v4.3$ smaller. In our study, the slower τ values as well as the slow recovery from inactivation observed in Endo support this.

Biophysical Analysis of I_{to} in the Left Ventricle

The electrophysiological properties of $K_v4.3$ channels are modulated by several β-subunits including KChIP2, which increases peak $K_v4.3$ current density, accelerates recovery from inactivation, and slows the decay (τ) of the current [16]. In the present study we demonstrated that the effect of NS5806 on heterologously expressed $K_v4.3$ channels is dependent on KChIP2. Epi and Mid cells had the highest KChIP2 levels and exhibited the largest I_{to} (Figure 2). Interestingly, the t of decay was faster in Epi and Mid than in Endo as also previously reported [5,32,33]. As KChIP2 slows $K_v4.3$ current decay, these findings may suggest that Endo I_{to} is not merely $K_v4.3$ in absence of KChIP2 and suggests that other subunits may contribute to Endo I_{to}. In further support of this notion is the observation that the decay of I_{to} in Epi, Mid and Endo was slowed by NS5806 suggesting that KChIP2 is a functional component of the I_{to} channels all three cell layers. The currents generated by $K_v4.3$ and KChIP2 channels did not recapitulate all the features of the native I_{to}. This is particularly evident when comparing the effect of NS5806 on recovery from inactivation. As also previous studies have demonstrated [5,32,33], the recovery from inactivation is much slower of Endo I_{to} than of Epi or Mid. The recovery of Epi and Mid I_{to} was accelerated by NS5806 whereas Endo I_{to} was unaffected. In contrast, NS5806 slowed recovery for heterologously expressed Kv4.3 independently of co-expression with KChIP2.

In agreement with previous publications, we found that KChIP2 increased Kv4.3 currents in both CHO-K1 cells and *Xenopus laevis* oocytes. The qPCR demonstrated a low abundance of KChIP2 in the endocardium and this would suggest less Kv4.3 mediated current. As the distribution of $K_V1.4$ and $K_V1.5$ message is uniform across the ventricular wall this would

likely result in a greater relative contribution of current mediated by $K_V1.4$ and $K_V1.5$ channels to endocardial I_{to}. It is tempting to speculate that the relatively larger contribution from $K_V1.4$ or $K_V1.5$ channels to Endo I_{to} compared to Epi and Mid I_{to} accounts for the differences in current kinetics as well as response to NS5806.

In summary, we have identified a novel I_{to} activator that appears to have differential effect on $I_{Kv4.3}$ in the presence or absence of KChIP2. Application of this compound to canine ventricular cells resulted in a differential augmentation on I_{to}. Our results suggest that the KChIP2 gradient is mainly responsible for the I_{to} gradient observed in the canine left ventricle. Since Epi and Mid cells have the highest KChIP2 levels, application of NS5806 had the largest effect on the decay of I_{to} and produced the largest increase in I_{to} in those 2 cell layers.

Acknowledgments

We are grateful to Judy Hefferon, Art Iodice, Trine Christiansen and Bob Goodrow for excellent technical assistance.

FUNDING SOURCES

This work was supported by grants from the Carlsberg Foundation [2006010173 to KC]; the American Health Assistance Foundation [JMC]; the Danish National Research Foundation [SPO]; the National Institutes of Health [HL47678 to CA] and the Masons of New York State and Florida.

Reference List

1. Antzelevitch, C.; Dumaine, R. Electrical heterogeneity in the heart: Physiological, pharmacological and clinical implications. In: Page, E.; Fozzard, HA.; Solaro, RJ., editors. Handbook of Physiology. Section 2 The Cardiovascular System. Oxford University Press; New York: 2001. p. 654-692.
2. Fedida D, Giles WR. Regional variations in action potentials and transient outward current in myocytes isolated from rabbit left ventricle. J Physiol 1991;442:191–209. [PubMed: 1665856]
3. Liu DW, Gintant GA, Antzelevitch C. Ionic bases for electrophysiological distinctions among epicardial, midmyocardial, and endocardial myocytes from the free wall of the canine left ventricle. Circ Res 1993;72:671–687. [PubMed: 8431990]
4. Campbell DL, Rasmusson RL, Qu YH, Strauss HC. The calcium-independent transient outward potassium current in isolated ferret right ventricular myocytes. I. Basic characterization and kinetic analysis. J Gen Physiol 1993;101:571–601. [PubMed: 8505627]
5. Wettwer E, Amos GJ, Posival H, Ravens U. Transient outward current in human ventricular myocytes of subepicardial and subendocardial origin. Circ Res 1994;75:473–482. [PubMed: 8062421]
6. Kuo HC, Cheng CF, Clark RB, Lin JJ, Lin JL, Hoshijima M, et al. A Defect in the Kv Channel-Interacting Protein 2 (KChIP2) Gene Leads to a Complete Loss of I(to) and Confers Susceptibility to Ventricular Tachycardia. Cell 2001;107:801–813. [PubMed: 11747815]
7. Deschênes I, DiSilvestre D, Juang GJ, Wu RC, An WF, Tomaselli GF. Regulation of $K_V4.3$ current by KChIP2 splice variants: a component of native cardiac I_{to}? Circulation 2002;106:423–429. [PubMed: 12135940]
8. Costantini DL, Arruda EP, Agarwal P, Kim KH, Zhu Y, Zhu W, et al. The homeodomain transcription factor Irx5 establishes the Mouse cardiac ventricular repolarization gradient. Cell 2005;123:347–358. [PubMed: 16239150]
9. Rossow CF, Minami E, Chase EG, Murry CE, Santana LF. NFATc3-induced reductions in voltage-gated K+ currents after myocardial infarction. Circ Res 2004;94:1340–1350. [PubMed: 15087419]
10. Radicke S, Cotella D, Graf EM, Ravens U, Wettwer E. Expression and function of dipeptidyl-aminopeptidase-like protein 6 as a putative beta-subunit of human cardiac transient outward current encoded by Kv4.3. J Physiol 2005;565:751–756. [PubMed: 15890703]
11. Zhang M, Jiang M, Tseng GN. minK-related peptide 1 associates with Kv4.2 and modulates its gating function: potential role as beta subunit of cardiac transient outward channel? Circ Res 2001;88:1012–1019. [PubMed: 11375270]

12. Radicke S, Cotella D, Graf EM, Banse U, Jost N, Varro A, et al. Functional modulation of the transient outward current Ito by KCNE b-subunits and regional distribution in human non-failing and failing hearts. Cardiovasc Res 2006;71:695–703. [PubMed: 16876774]
13. Dixon EJ, Shi W, Wang H-S, McDonald C, Yu H, Wymore RS, et al. Role of the Kv4.3 K+ channel in ventricular muscle. A molecular correlate for the transient outward current. Circ Res 1996;79:659–668. [PubMed: 8831489]
14. Sridhar A, da Cunha DN, Lacombe VA, Zhou Q, Fox JJ, Hamlin RL, et al. The plateau outward current in canine ventricle, sensitive to 4-aminopyridine, is a constitutive contributor to ventricular repolarization. Br J Pharmacol 2007;152:870–879. [PubMed: 17700726]
15. Rosati B, Pan Z, Lypen S, Wang HS, Cohen I, Dixon JE, et al. Regulation of KChIP2 potassium channel beta subunit gene expression underlies the gradient of transient outward current in canine and human ventricle. J Physiol 2001;533:119–125. [PubMed: 11351020]
16. Rosati B, Grau F, Rodriguez S, Li H, Nerbonne JM, McKinnon D. Concordant expression of KChIP2 mRNA, protein and transient outward current throughout the canine ventricle. J Physiol 2003;548:815–822. [PubMed: 12598586]
17. Zicha S, Xiao L, Stafford S, Cha TJ, Han W, Varro A, et al. Transmural expression of transient outward potassium current subunits in normal and failing canine and human hearts. J Physiol 2004;561:735–748. [PubMed: 15498806]
18. Calloe K, Cordeiro JM, Di Diego JM, Hansen RS, Grunnet M, Olesen SP, et al. A transient outward potassium current activator recapitulates the electrocardiographic manifestations of Brugada syndrome. Cardiovasc Res 2009;81:686–694. [PubMed: 19073629]
19. Cordeiro JM, Greene L, Heilmann C, Antzelevitch D, Antzelevitch C. Transmural heterogeneity of calcium activity and mechanical function in the canine left ventricle. Am J Physiol Heart Circ Physiol 2004;286:H1471–H1479. [PubMed: 14670817]
20. Cordeiro JM, Malone JE, Di Diego JM, Scornik FS, Aistrup GL, Antzelevitch C, et al. Cellular and subcellular alternans in the canine left ventricle. Am J Physiol Heart Circ Physiol 2007;293:H3506–H3516. [PubMed: 17906109]
21. Dumaine R, Cordeiro JM. Comparison of K(+) currents in cardiac Purkinje cells isolated from rabbit and dog. J Mol Cell Cardiol 2007;42:378–389. [PubMed: 17184792]
22. Livak KJ, Schmittgen TD. Analysis of relative gene expression data using real-time quantitative PCR and the 2(-Delta Delta C(T)) Method. Methods 2001;25:402–408. [PubMed: 11846609]
23. Han W, Bao W, Wang Z, Nattel S. Comparison of ion-channel subunit expression in canine cardiac Purkinje fibers and ventricular muscle. Circ Res 2002;91:790–797. [PubMed: 12411393]
24. Costantini DL, Arruda EP, Agarwal P, Kim KH, Zhu Y, Zhu W, et al. The homeodomain transcription factor Irx5 establishes the Mouse cardiac ventricular repolarization gradient. Cell 2005;123:347–358. [PubMed: 16239150]
25. Rosati B, Grau F, McKinnon D. Regional variation in mRNA transcript abundance within the ventricular wall. J Mol Cell Cardiol 2006;40:295–302. [PubMed: 16412459]
26. Decher N, Uyguner O, Scherer CR, Karaman B, Yuksel-Apak M, Busch AE, et al. hKChIP2 is a functional modifier of hKv4.3 potassium channels: cloning and expression of a short hKChIP2 splice variant. Cardiovasc Res 2001;52:255–264. [PubMed: 11684073]
27. Akar FG, Wu RC, Deschênes I, Armoundas AA, Piacentino V III, Houser SR, et al. Phenotypic differences in transient outward K^+ current of human and canine ventricular myocytes: insights into molecular composition of ventricular I_{to}. Am J Physiol Heart Circ Physiol 2004;286:H602–H609. [PubMed: 14527940]
28. Deschênes I, Tomaselli GF. Modulation of $K_V4.3$ current by accessory subunits. FEBS Lett 2002;528:183–188. [PubMed: 12297301]
29. Lundby A, Olesen SP. KCNE3 is an inhibitory subunit of the Kv4.3 potassium channel. Biochem Biophys Res Commun 2006;346:958–967. [PubMed: 16782062]
30. Delpón E, Cordeiro JM, Núñez L, Thomsen PEB, Guerchicoff A, Pollevick GD, et al. Functional effects of *KCNE3* mutation and its role in the development of Brugada syndrome. Circ Arrhythm Electrophysiol 2008;1:209–218. [PubMed: 19122847]

31. Fedida D, Eldstrom J, Hesketh JC, Lamorgese M, Castel L, Steele DF, et al. Kv1.5 is an important component of repolarizing K^+ current in canine atrial myocytes. Circ Res 2003;93:744–751. [PubMed: 14500335]

32. Brahmajothi MV, Campbell DL, Rasmusson RL, Morales MJ, Trimmer JS, Nerbonne JM, et al. Distinct transient outward potassium current (Ito) phenotypes and distribution of fast-inactivating potassium channel alpha subunits in ferret left ventricular myocytes. J Gen Physiol 1999;113:581–600. [PubMed: 10102938]

33. Yu H, Gao J, Wang H, Wymore R, Steinberg S, McKinnon D, et al. Effects of the renin-angiotensin system on the current I(to) in epicardial and endocardial ventricular myocytes from the canine heart. Circ Res 2000;86:1062–1068. [PubMed: 10827136]

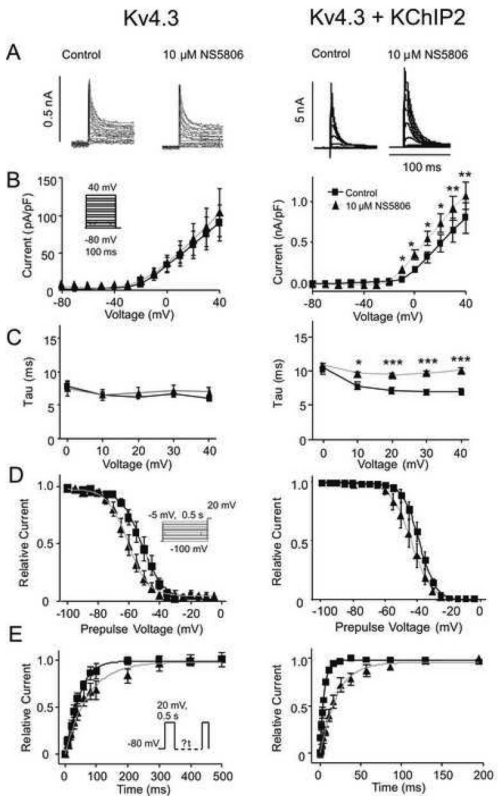

Figure 1.

A: Representative traces of $K_V4.3$ currents recorded in the absence (left, n=6) and presence of KChIP2 (right, n=5-10) under control conditions and in presence of 10 μM NS5806. From a holding potential of −80 mV, cells were stepped to +40 mV in 10 mV increments. **Panel B:** Mean I-V relations for peak current density **Panel C:** Mean τ's in absence and presence of NS5806. **Panel D:** Voltage dependence of inactivation and Boltzmann curves showing mid-inactivation **Panel E:** Time-dependent recovery from inactivation was evaluated using a standard double pulse protocol from a holding of −80 mV.

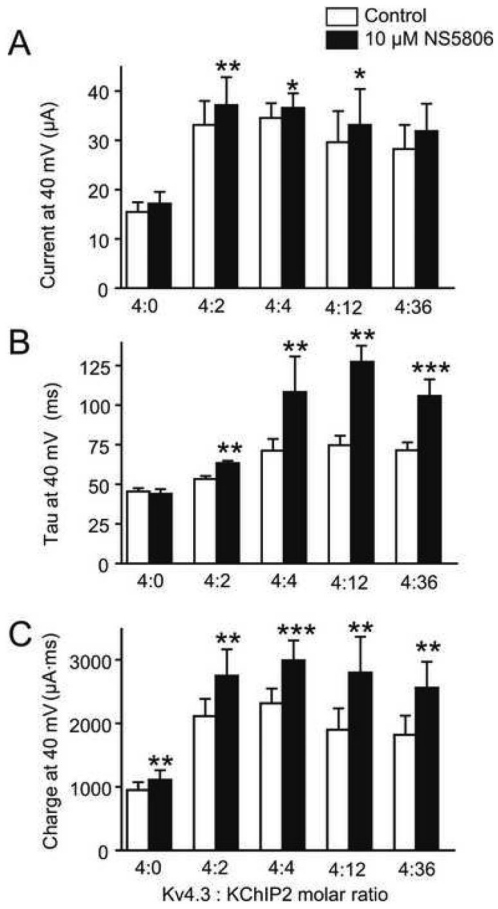

Figure 2.

The effect of NS5806 on different ratios of $K_v4.3$ and KChIP2 expressed in *Xenopus laevis* oocytes. Mean data showing peak current **(Panel A),** decay (τ) of the current **(Panel B)** and total charge **(Panel C)**. n=7-8 oocytes

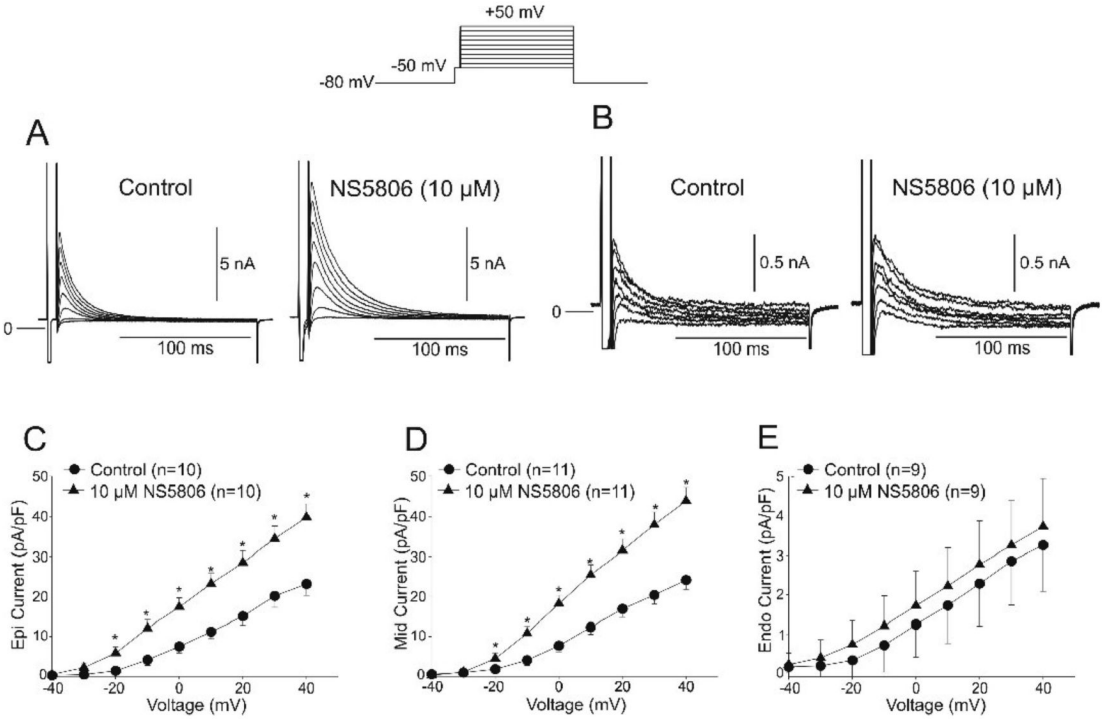

Figure 3.

Representative I_{to} traces recorded from an Epi **(Panel A)** and an Endo cell **(Panel B)** under control conditions and in the presence of NS5806 (10 μM). The voltage clamp protocol is shown at the top of the figure and Cd^{2+} was present to block I_{CaL}. Mean I-V relation for peak I_{to} from Epi **(Panel C)**, Mid **(Panel D)** and Endo cells **(Panel E)** in absence and presence of NS5806 (10μM). The density of I_{to} was greater in Epi and Mid cells and application of NS5806 caused a substantial increase in the magnitude of I_{to}.

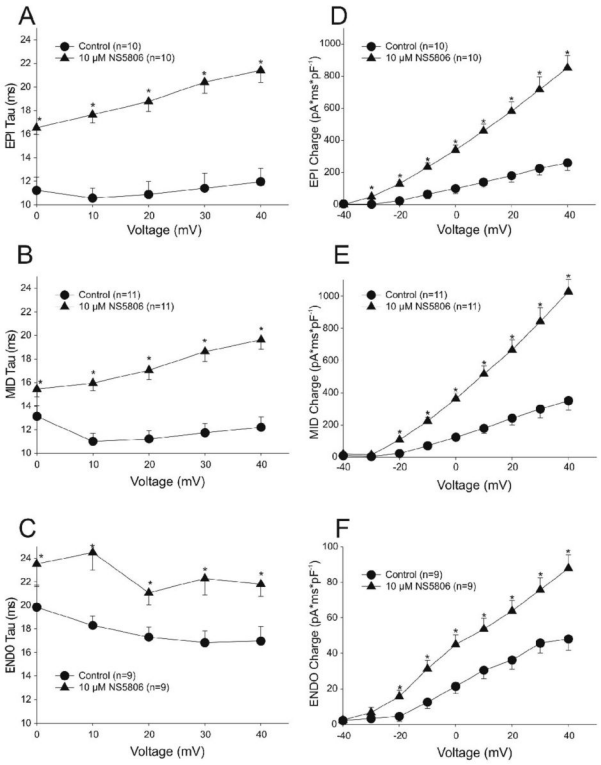

Figure 4.

I_{to} decay as a function of voltage for Epi, Mid and Endo cells under control conditions and in the presence of NS5806 (10 μM) **(Panels A-C)**. **Panels D-F:** Total I_{to} charge (area under the curve) was increased by NS5806 in all 3 cell layers.

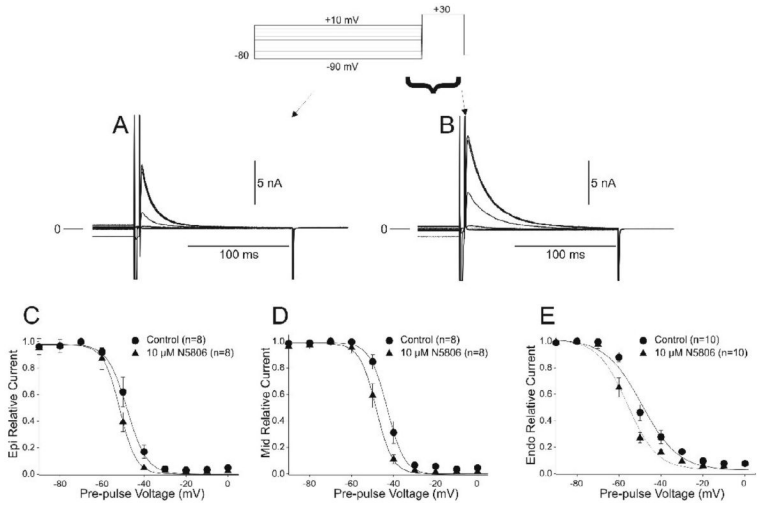

Figure 5.

Representative traces recorded under control conditions (**Panel A**) and after application of 10 μM NS5806 (**Panel B**) showing voltage dependence of inactivation of I_{to}. Boltzmann curves showing mid-inactivation voltages for Epi (**Panel C**), Mid (**Panel D**) and Endo (**Panel E**) cells in the absence and presence of drug.

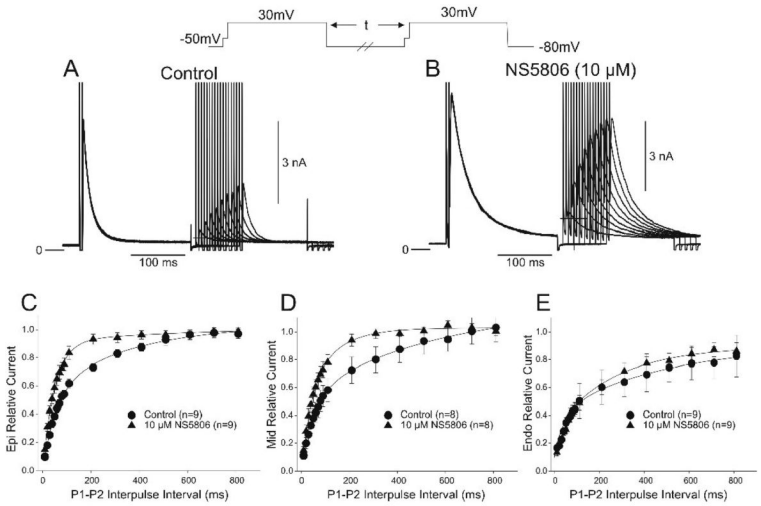

Figure 6.

Representative traces recorded under control conditions (**Panel A**) and after 10 μM NS5806 (**Panel B**) showing recovery of I_{to}. Cd^{2+} was present to block I_{CaL}. The recovery time-course of I_{to} recorded from Epi (**Panel C**), Mid (**Panel D**) and Endo (**Panel E**) cells in the absence and presence of drug.

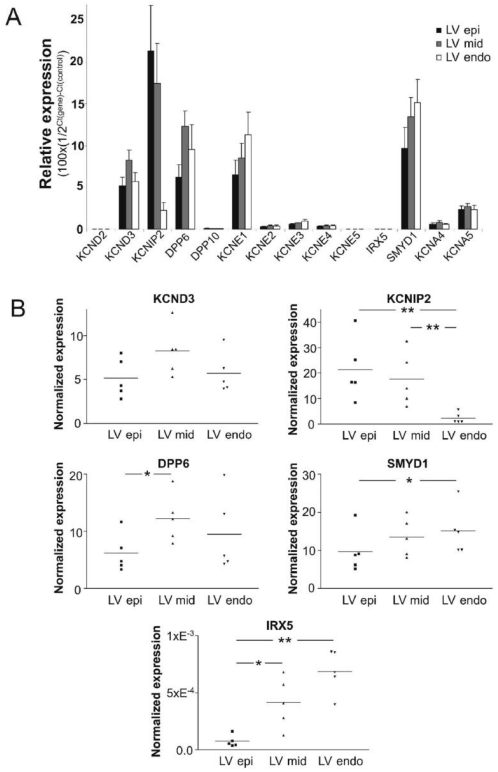

Figure 7.

qPCR of left ventricular canine tissue. Epi, Mid, and Endo tissue was isolated from 5 canine left ventricles. Taqman based assays (Applied Biosystems) were used to quantify mRNA of interest which was then normalized to *cyclophilin B* expression **(Panel A).** Dot plots of *KCND3*, *KCNIP2*, *DPP6*, *IRX5*, and *SMYD1* expression **(Panel B)**. The expression level values were obtained as described in materials and methods.

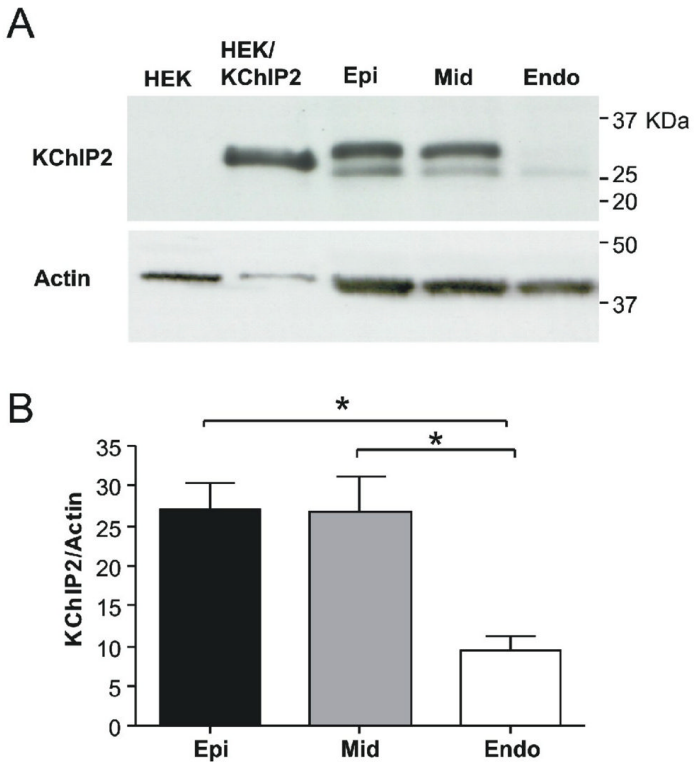

Figure 8.

A: Transmural gradient of KChIP2 protein in canine left ventricle. Representative blot of KChIP2 expression in Endo-, Mid- and Epi. KChIP2 expressing and non-transfected HEK-293 cell lysates were included as controls. For Epi, Mid and Endo, two bands sized 25-32 kDa were consistently detected for all protein isolation methods tested. The same blot was re-probed with anti-actin antibody. **Panel B:** Both KChIP2 bands were quantified and KChIP2 expression normalized to actin expression. Tissue from 5 dogs was analysed.